*Journal of the Korean Chemical Society*
**2013**, *Vol. 57, No. 1*
Printed in the Republic of Korea
http://dx.doi.org/10.5012/jkcs.2013.57.1.12

# Single-Crystal Structure of $|Li_{50}Na_{25}|[Si_{117}Al_{75}O_{384}]$-FAU

**Hu Sik Kim, Jeong Min Suh†, Jum Soon Kang‡, and Woo Taik Lim***

*Department of Applied Chemistry, Andong National University, Andong 760-749, Korea.*
**E-mail: wtlim@andong.ac.kr*
†*Department of Bioenvironmental Engergy, Pusan National University, Miryang 627-706, Korea*
‡*Department of Horticultural Bioscience, Pusan National University, Miryang 627-706, Korea*
(Received October 8, 2012; Accepted November 12, 2012)

**ABSTRACT.** The single-crystal structure of fully dehydrated partially $Li^+$-exchanged zeolite Y, $|Li_{50}Na_{25}|[Si_{117}Al_{75}O_{384}]$-FAU, was determined by single-crystal synchrotron X-ray diffraction techniques in the cubic space group $Fd\bar{3}m$ at 100(1) K. Ion exchange was accomplished by flowing stream of 0.1 M aqueous $LiNO_3$ for 2 days at 293 K, followed by vacuum dehydration at 623 K and $1\times10^{-6}$ Torr for 2 days. The structure was refined using all intensities to the final error indices (using only the 801 reflections with ($F_o > 4\sigma(F_o)$) $R_1/R_2 = 0.043/0.140$. The 50 $Li^+$ ions per unit cell are found at three different crystallographic sites. The 19 $Li^+$ ions occupy at site I' in the sodalite cavity: the $Li^+$ ions are recessed 0.30 Å into the sodalite cavity from their 3-oxygens plane (Li–O = 1.926(5) Å and O–Li–O = 117.7(3)°). The 20 $Li^+$ ions are found at site II in the supercage, being recessed 0.23 Å into the supercage (Li–O = 2.038(5) Å and O–Li–O = 118.7(3)°). Site III' positions are occupied by 11 $Li^+$ ions: these $Li^+$ ions bind strongly to one oxygen atom (Li–O = 2.00(8) Å). About 25 $Na^+$ ions per unit cell are found at four different crystallographic sites: 4 $Na^+$ ions are at site I, 5 at site I', 12 at site II, and the remaining 4 at site III'.

**Key words:** Lithium, Zeolite Y, Ion exchange, Structure, Dehydrated

## INTRODUCTION

Faujasite-type zeolites (FAU) are widely used in the range of applications as gas sorption, gas separation, and effective catalysts for many chemical reactions due to the excellent stability of the crystal structure and pore system.[1–4] These processes depend on the type, number, and distribution of exchangeable cations over the available sites.[5] Generally, the sorption property of zeolite is related to the forces of interaction between the sorbate molecules and the zeolite. Smaller cations with higher charges will render a zeolite more effective as a sorbing agent.[6]

The $Li^+$ ion is so small and it charge more concentrated. Accordingly, fully dehydrated fully $Li^+$-exchanged zeolites are generally used in the separation of nitrogen from air in the PSA (pressure swing adsorption) process.[7–9] In addition, $Li^+$-exchanged faujasite-type zeolites are useful as microporous catalysts for industrially important reactions such as ring alkylation of toluene[10] and isomerization of olefins.[11]

The crystal structures of $Li^+$-exchanged faujasite-type zeolites have been widely studied by several scientists for the understanding of their properties.[12–15] However, it is not easy to study local structure of $Li^+$ ions because of their low X-ray scattering power and mobility in the supercage of zeolite.

Forano et al. investigated the dehydrated partially $Li^+$-exchanged zeolites X (Si/Al = 1.23) and Y (Si/Al = 2.36) by powder neutron diffraction techniques.[12] They tried to improve the degree of $Li^+$ exchange into zeolites X and Y using $NH_4^+$-X and Y because the more loosely bound $NH_4^+$ ion as compared to $Na^+$ would be more easily replaced by $Li^+$ ion.[16] However, both $Na^+$ and $H^+$ ions were found in these structures.

Plevert et al. studied the fully dehydrated $Li^+$-exchanged zeolite X (Si/Al = 1.0) at two different temperatures of 300 and 10 K by powder neutron diffraction techniques.[13] They reported that a phase transition was occurred at low temperature from $Fd\bar{3}$(cubic) to *Fddd* (orthorhombic) due to the large distortion of the framework by the strong interaction between $Li^+$ ions and the framework oxygen atoms.

Lobo et al. also investigated the phase transition in fully dehydrated fully $Li^+$-exchanged zeolites X (Si/Al = 1.0 and 1.25) by solid-state MAS NMR spectroscopy and neutron diffraction technique.[14] Phase transition from $Fd\bar{3}$ to *Fddd* was observed in the temperature range T = 200–300 K in the structure of Li-X (Si/Al = 1.0). However, it was interesting that phase transition did not occur at low temperature (10 K) in Li-X (Si/Al = 1.25).

Smolin et al. studied that the structures of the hydrated and partially dehydrated a partially $Li^+$-exchanged zeolites X by single-crystal X-ray diffraction techniques to

explore the detailed knowledge of the structure and chemical compositions.[15] However, the informations of $Li^+$ and $Na^+$ ions in both structures were incomplete. In addition, the structure determination of fully dehydrated $Li^+$-exchanged zeolite X was failed due to the loss of crystallinity at high dehydration temperature.

According to the previous studies of dehydrated Li-LSX,[13,14] Li-X (Si/Al = 1.23 and 1.25),[12,14] and Li-Y (Si/Al = 1.56),[17] $Li^+$ ions tend to occupy preferentially sites I' and II and the remaining $Li^+$ ions were located at site III or III' in the supercage. Sometimes it was not found crystallographically, because of their low occupancies and scattering powers at sites III or III'.

In the case of Li-LSX, [13] $Li^+$ ions were equally located at sites III and III', respectively. Unlike the Li-LSX,[13] $Li^+$ ions were found only at site III' in Li-LSX, Li-X (Si/Al = 1.25),[14] Li-X (Si/Al = 1.23),[12] and Li-Y (Si/Al = 1.56),[17] but were not found at site III.

Generally, the complete exchange of $Li^+$ for $Na^+$ ion was readily achieved for LSX (Si/Al = 1.0) from conventional aqueous solution.[13,14] However, it is not simple to achieve completely $Li^+$-exchanged zeolite when Si/Al ratio was higher than 1.0.[12,14,17]

Composition of zeolite Y (Si/Al = 1.56) is quite different to those of the previous structures. It would show unique application in separation and catalysis due to the different distribution and coordination of $Li^+$ ions by different the local Si/Al ordering in tetrahedral sites. Therefore, knowledge of the distribution of $Li^+$ ions in the zeolite Y framework is a key for understanding of peoperties of the $Li^+$ ions.

This work was carried out to investigate the precise cation position of $Li^+$ and $Na^+$ ions in fully dehydrated partially $Li^+$-exchanged zeolite Y (FAU, Si/Al = 1.56) from conventional aqueous solution at room temperature by single-crystal synchrotron X-ray diffraction techniques. Previous reports for the structures of $Li^+$-exchanged faujasite-type zeolites will be compared with that from our results.

## EXPERIMENTAL SECTION

### Ion Exchange of Zeolite Y (FAU)

Large single crystals of zeolite Y (FAU), stoichiometry $Na_{75}Si_{117}Al_{75}O_{384}$, were synthesized in this laboratory.[18] One crystal, colorless octahedra about 0.18 mm in cross-section, was lodged in a fine Pyrex capillary. Ion exchange was accomplished at 293 K by flowing stream of 0.1 M aqueous $LiNO_3$ (Aldrich, 99.99%, Ca 4.82 ppm, Na 1.91 ppm, Sc 0.48 ppm, Mg 0.42 ppm, Ba 0.41 ppm, Zr 0.31 ppm, Cu 0.21 ppm, Al 0.07 ppm, La 0.05 ppm, Sr 0.04 ppm). The resulting clear colorless single crystal was slowly heated under dynamic vacuum to 673 K and dehydrated at $1 \times 10^{-6}$ Torr for two days. While these conditions were maintained, the hot contiguous downstream lengths of the vacuum system, including a sequential 17 cm U-tube of zeolite 5A beads fully activated in situ, were allowed to cool to ambient temperature to prevent the movement of water molecules from more distant parts of the vacuum system to the crystal. While still under vacuum, the crystal was allowed to cool to room temperature and was sealed in its capillary by torch. Microscopic examination showed them to be colorless.

### Single-crystal X-ray Diffraction Work

X-ray diffraction data for the crystal was collected at 100(1) K using an ADSC Quantum 210 detector at Beamline 6B MXI at The Pohang Light Source. For crystal, the preliminary cell constants and an orientation matrix were determined from 36 sets of frames collected at scan intervals of 5 with an exposure time of 1 second per frame. The basic data file was prepared using the program HKL2000.[19] The reflections were successfully indexed by the auto-

***Table* 1.** Summary of experimental and crystallographic data

| | $\|Li_{50}Na_{25}\|[Si_{117}Al_{75}O_{384}]$-FAU |
|---|---|
| Crystal cross-section (mm) | 0.18 |
| Ion exchange t(h),T (K) | 48, 293 |
| Crystal color | colorless |
| Dehydration T (K) | 673 |
| Data collection T (K) | 100(1) |
| Space Group, Z | $Fd\bar{3}m$, 1 |
| X-ray source | Pohang Light Source, Beamline 6B MXI |
| Wavelength (Å) | 0.90000 |
| Unit cell constant, $a$ (Å) | 24.6660(1) |
| 2θ range in data collection (deg) | 70.47 |
| No. of unique reflections, $m$ | 838 |
| No. of reflections with $F_o > 4\sigma(F_o)$ | 801 |
| No. of variables, $s$ | 63 |
| Data/parameter ratio, $m/s$ | 13.3 |
| Weighting parameters, $a/b$ | 0.054/118.8 |
| Final error indices | |
| $R_1/wR_2$ ($F_o > 4\sigma(F_o)$)[a] | 0.043/0.140 |
| $R_1/wR_2$ (all intensities)[b] | 0.044/0.145 |
| Goodness-of-fit[c] | 1.30 |

[a] $R_1 = \Sigma||F_o|-|F_c||/\Sigma F_o$ and $R_2 = [\Sigma w(F_o^2-F_c^2)^2/\Sigma w(F_o^2)^2]^{1/2}$; $R_1$ and $R_2$ are calculated using only the 801 reflections for which $F_o > 4\sigma(F_o)$. [b] $R_1$ and $R_2$ are calculated using all unique reflections measured. [c] Goodness-of-fit = $(\Sigma w(F_o^2-F_c^2)^2/(m-s))^{1/2}$, where $m$ and $s$ are the number of unique reflections and variables, respectively

mated indexing routine of the DENZO program.[19] The diffraction intensities were harvested by collecting 72 sets of frames with 5 scans and an exposure time of 1 second per frame. These highly redundant data sets were corrected for Lorentz and polarization effects; negligible corrections for crystal decay were also applied.

The space group $Fd\bar{3}m$, conventional for zeolite Y, was determined by the program XPREP.[20] Additional experimental details are presented in *Table* 1.

## STRUCTURE DETERMINATION

Full-matrix least-squares refinements (SHELXL97)[21] were done on $F_o^2$ using all data. Refinement was initiated with the atomic parameters of the framework atoms [(Si, Al), O(1), O(2), O(3), and O(4)] in dehydrated $|K_{71}|[Si_{121}Al_{71}O_{384}]$-FAU.[22] Initial refinement used anisotropic thermal parameters and converged to the error indices given in steps 1 of *Table* 2. The detailed progress of structure determination as subsequent peaks were found on difference Fourier functions and identified as nonframework atoms is provided in *Table* 2. The final cycles of refinement were done with anisotropic temperature factors for all positions except those that were not stable in anisotropic refinement: Na (I'), Li(II), and Li(III'). The final error indices $R_1$ and $R_2$ are given in *Table* 1. The largest peaks on the final difference-Fourier function were not included in the final model because they were too far from framework oxygen

***Table* 2.** Steps of structure refinement[a]

| | Occupancy[b] at | | | | | | | | |
|---|---|---|---|---|---|---|---|---|---|
| Step | Na(I) | Li(I') | Na(I') | Li(II) | Na(II ) | Li(III') | Na(III') | $R_1$ | $R_2$ |
| 1[c] | | | | | | | | 0.1343 | 0.3596 |
| 2 | | | | | 12.3(8) | | | 0.1029 | 0.2837 |
| 3 | 3.2(4) | | | | 13.7(6) | | | 0.0672 | 0.1926 |
| 4 | 3.0(3) | 39.8(24) | | | 14.8(5) | | | 0.0606 | 0.1822 |
| 5 | 3.1(2) | 41.1(22) | | 29.4(34) | 8.5(7) | | | 0.0539 | 0.1669 |
| 6 | 3.2(2) | 25.6(31) | 3.8(7) | 28.4(32) | 8.9(7) | | | 0.0488 | 0.1571 |
| 7 | 3.4(2) | 25.4(32) | 3.8(7) | 29.3(32) | 9.3(7) | 15.6(54) | | 0.0485 | 0.1552 |
| 8 | 3.7(2) | 27.0(32) | 3.9(7) | 31.5(32) | 9.3(7) | 11.3(44) | 3.7(6) | 0.0436 | 0.1427 |
| 9[d] | 3.7(2) | 19.6(4) | 5.1(4) | 30.9(32) | 9.3(7) | 11.3(44) | 3.5(6) | 0.0439 | 0.1432 |
| 10[e] | 3.7(2) | 19.7(4) | 4.9(4) | 21.2(4) | 10.8(4) | 9.7(40) | 3.3(6) | 0.0445 | 0.1441 |
| 11[f] | 3.8(2) | 19.5(4) | 5.2(4) | 19.6(4) | 12.4(4) | 13(4) | 3.7(6) | 0.0427 | 0.1403 |

[a]Isotropic temperature factors were used for all $Li^+$ and $Na^+$ positions except for the last step. [b]The occupancy is given as the number of $Li^+$ and $Na^+$ ions per unit cell. [c]Only the atoms of zeolite framework were included in the initial structure model. [d]Occupancies at sites I and I' constrained so that $n_I + n_{I'}/2 \leq 16$. [e]Constrained to sum to 32, the maximum occupancy at site II. [f]$Li^+$ and $Na^+$ ions were refined anisotropically, except Na(I'), Li(II), and Li(III').

***Table* 3.** Positional, thermal, and occupancy parameters

| Atom | Wyckoff position | Cation site | x | y | z | [b]$U_{11}$ or $U_{iso}$ | $U_{22}$ | $U_{33}$ | $U_{23}$ | $U_{13}$ | $U_{12}$ | [c]Occupancy | | |
|---|---|---|---|---|---|---|---|---|---|---|---|---|---|---|
| | | | | | | | | | | | | initial | varied | fixed |
| Si, Al | 192(*i*) | | −506(1) | 1234(1) | 378(1) | 409(8) | 380(8) | 377(8) | −24(5) | −5(5) | −14(5) | 192 | | |
| O(1) | 96(*h*) | | −972(2) | −7(2) | 1021(2) | 473(21) | 515(22) | 448(20) | −34(16) | −38(16) | −61(17) | 96 | | |
| O(2) | 96(*g*) | | 1(1) | 15(1) | 1529(1) | 368(17) | 380(17) | 431(19) | −9(14) | −12(14) | 43(14) | 96 | | |
| O(3) | 96(*g*) | | −700(2) | −741(2) | 204(2) | 415(18) | 421(19) | 490(21) | 22(16) | 32(16) | 54(15) | 96 | | |
| O(4) | 96(*g*) | | −732(2) | 779(1) | 1689(1) | 422(19) | 424(19) | 428(19) | −79(15) | −5(15) | −27(15) | 96 | | |
| Na(I) | 16(*c*) | I | 0 | 0 | 0 | 84(40) | 84(40) | 84(40) | 2(26) | 2(26) | 2(26) | | 3.8(2) | 4 |
| Li(I') | 32(*e*) | I' | 469(5) | 469(5) | 469(5) | 115(32) | 115(32) | 115(32) | −12(45) | −12(45) | −12(45) | | 19.5(4) | 19 |
| Na(I') | 32(*e*) | I' | 598(7) | 598(7) | 598(7) | 394(84) | | | | | | | 5.2(4) | 5 |
| Li(II) | 32(*e*) | II | 2223(7) | 2223(7) | 2223(7) | 352(74) | | | | | | | 19.6(4) | 20 |
| Na(II) | 32(*e*) | II | 2375(4) | 2375(4) | 2375(4) | 423(37) | 423(37) | 423(37) | 225(41) | 225(41) | 225(41) | | 12.4(4) | 12 |
| Li(III') | 192(*i*) | III' | 706(74) | 822(73) | 4018(49) | 821(564) | | | | | | | 13(4) | 11 |
| Na(III') | 192(*i*) | III' | 1024(13) | 147(13) | 3970(15) | 121(187) | 357(172) | 357(172) | −136(176) | 147(120) | −147(120) | | 3.7(6) | 4 |

[a]Positional parameters × $10^4$ and thermal parameters × $10^4$ are given. Numbers in parentheses are the estimated standard deviations in the units of the least significant figure given for the corresponding parameter. [b]The anisotropic temperature factor is $\exp[-2\pi^2 a^{-2}(U_{11}h^2 + U_{22}k^2 + U_{33}l^2 + 2U_{23}kl + 2U_{13}hl + 2U_{12}hk)]$. [c]Occupancy factors are given as the number of atoms or ions per unit cell.

***Table* 4.** Selected interatomic distances (Å) and angles (deg)[a]

| | Distances | | Angles |
|---|---|---|---|
| (Si,Al)-O(1) | 1.6319(11) | O(1)-(Si,Al)-O(2) | 113.05(11) |
| (Si,Al)-O(2) | 1.6791(13) | O(1)-(Si,Al)-O(3) | 108.97(13) |
| (Si,Al)-O(3) | 1.6973(4) | O(1)-(Si,Al)-O(4) | 111.79(14) |
| (Si,Al)-O(4) | 1.6349(11) | O(2)-(Si,Al)-O(3) | 104.90(13) |
| **Mean (Si,Al)** | **1.661(3)** | O(2)-(Si,Al)-O(4) | 107.05(13) |
| | | O(3)-(Si,Al)-O(4) | 110.87(14) |
| Na(I)-O(3) | 2.556(3) | | |
| Li(I')-O(3) | 1.926(5) | (Si,Al)-O(1)-(Si,Al) | 146.35(21) |
| Na(I')-O(3) | 2.083(12) | (Si,Al)-O(2)-(Si,Al) | 132.19(18) |
| Li(II)-O(2) | 2.038(5) | (Si,Al)-O(3)-(Si,Al) | 126.79(18) |
| Na(II)-O(2) | 2.211(7) | (Si,Al)-O(4)-(Si,Al) | 144.21(19) |
| Li(III')-O(4) | 2.00(12) | | |
| Na(III')-O(1) | 2.77(4), 2.77(4) | O(3)-Na(I)-O(3) | 80.3(1), 99.7(1) |
| Na(III')-O(4) | 2.60(3), 2.60(3) | O(3)-Li(I')-O(3) | 117.7(3) |
| | | O(3)-Na(I')-O(3) | 104.6(8) |
| | | O(2)-Li(II)-O(2) | 118.7(3) |
| | | O(2)-Na(II)-O(2) | 104.9(4) |
| | | O(4)-Na(III')-O(4) | 77.3(9) |

[a]The numbers in parentheses are the estimated standard deviations in the units of the least significant digit given for the corresponding parameter

atoms to be cations and were not otherwise within bonding distance of any other position. All shifts in the final cycles of refinements were less than 0.1% of their corresponding estimated standard deviations (esds). The final structural parameters are presented in *Table* 3 and selected interatomic distances and angles are given in *Table* 4.

Fixed weights were used initially; the final weights were assigned using the formula $w = 1/[\sigma^2(F_o^2) + (aP)^2 + bP]$ where $P = [\mathrm{Max}(F_o^2,0) + 2F_c^2]/3$, with $a$ and $b$ as refined parameters (see *Table* 1). Atomic scattering factors for $Li^+$, $Na^+$, $O^-$, and $(Si,Al)^{1.82+}$ were used.[23,24] The function describing $(Si, Al)^{1.82+}$ is a weighted (for composition) mean of the $Si^{4+}$, $Si^0$, $Al^{3+}$, and $Al^0$ functions (Si/Al = 1.56). All scattering factors were modified to account for anomalous dispersion.[25,26] Other crystallographic details are given in *Table* 1.

## RESULTS AND DISCUSSION

The framework structure of zeolite Y (FAU) is characterized by the double 6-ring (D6R, hexagonal prism), the sodalite cavity (a cubooctahedron), and the supercage (see *Fig.* 1). Each unit cell has 8 supercages, 8 sodalite cavities, 16 D6Rs (32 6-rings), 16 12-rings, and 32 single 6-rings (S6Rs).

The exchangeable cations, which balance the negative charges of the zeolite Y framework, usually occupy some or all of the sites shown with Roman numerals in *Fig.* 1. The maximum occupancies at the cation sites I, I', II, II', and III in zeolite Y are 16, 32, 32, 32, and 48, respectively. Site III' in zeolite Y studied using space group $Fd\bar{3}m$ is a 192-fold position. Further description is available.[28,29]

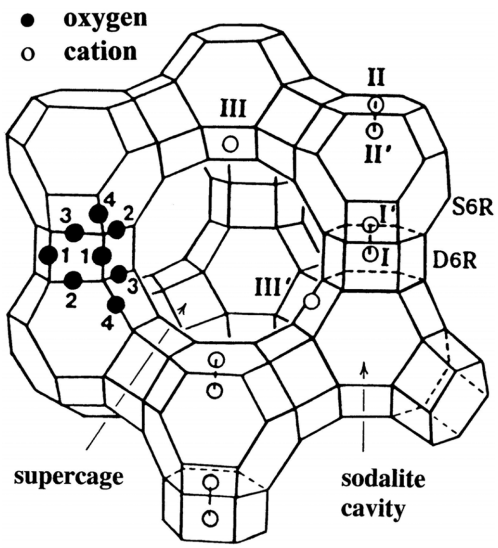


***Fig.* 1.** Stylized drawing of the framework structure of zeolite Y. Near the center of the each line segment is an oxygen atom. The different oxygen atoms are indicated by the numbers 1 to 4. There is no evidence in this work of any ordering of the silicon and aluminum atoms among the tetrahedral positions, although it is expected that Lowenstein's rule (ref. 26) would be obeyed. Extraframework cation positions are labeled with Roman numerals.

In this structure, 50 $Li^+$ ions per unit cell are found at sites I', II, and III' and 25 $Na^+$ ions at sites I, I', II, and III'

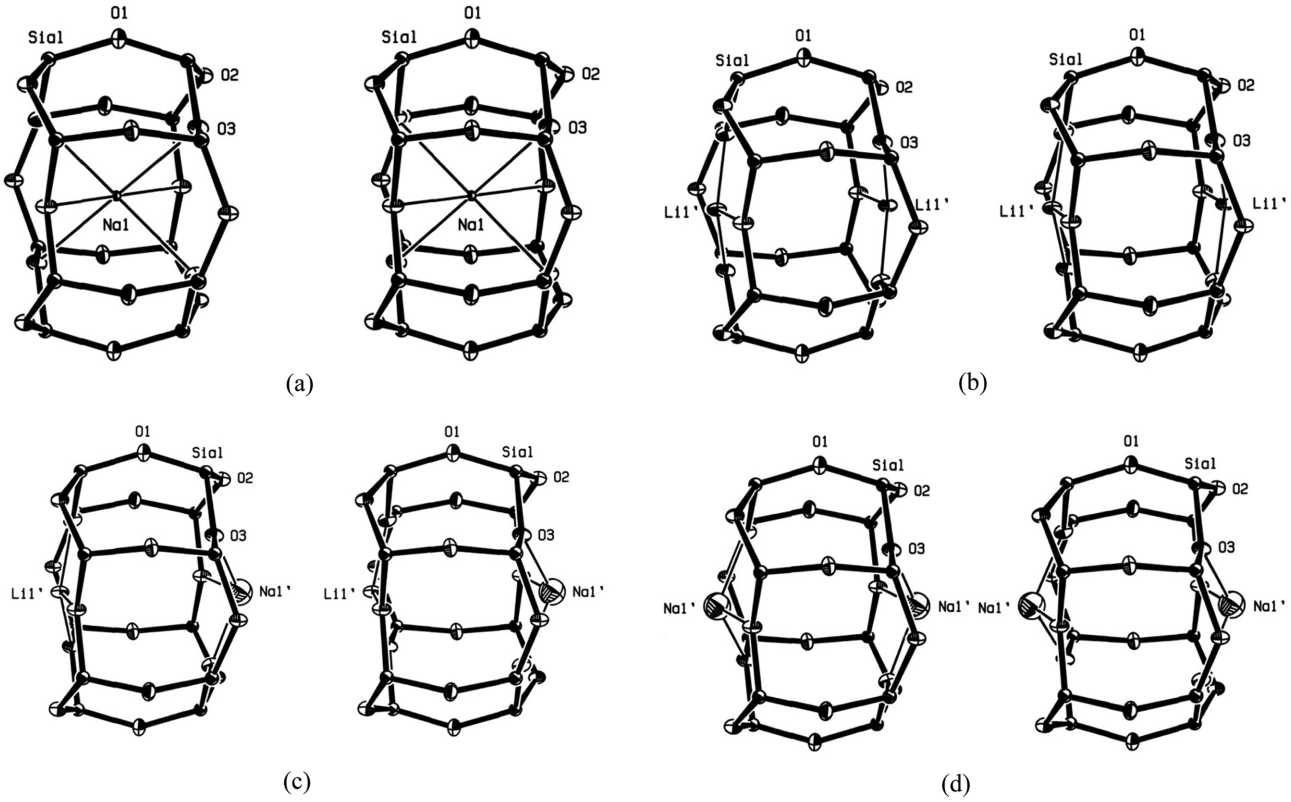


***Fig.* 2.** Stereoviews of the four possible ways that cations occupy double 6-rings (D6Rs) in dehydrated $|Li_{50}Na_{25}|[Si_{117}Al_{75}O_{384}]$-FAU. Of the 16 D6Rs per unit cell in dehydrated $|Li_{50}Na_{25}|$ $[Si_{117}Al_{75}O_{384}]$-FAU, four are occupied as shown in (a), nine as shown in (b), five as shown in (c), and two as shown in (d). The zeolite Y framework is drawn with heavy bonds. The coordination of $Li^+$ and $Na^+$ ions to oxygens of the zeolite framework is indicated by light bonds. Ellipsoids of 25% probability are shown.

(see *Table* 3). The degree of $Li^+$-ion exchange in this structure is therefore about 67%.

Four $Na^+$ ions per unit cell at Na(I) occupy site I (at the center of the D6Rs, see *Fig*. 2(a)). Each coordinates to six O(3) framework oxygens of its D6R at distance of 2.556(3) Å, which is much longer than the sum of the corresponding ionic radii, 0.97 + 1.32 = 2.29 Å,[30] indicating a reasonably good fit: this was seen before in the structure of $|Li_{54}Na_{21}|$ $[Si_{117}Al_{75}O_{384}]$-FAU.[17] The Na(I) is nearly octahedral with O(3)–Na(I)–O(3) bond angles at 80.3(1)° and 99.7(1)° (see *Table* 4). In this position, $Li^+$ ions do not fit in octahedral coordination at the center of the hexagonal prism due to small size of $Li^+$ ion.

The 19 $Li^+$ and 5 $Na^+$ ions at Li(I') and Na(I'), respectively, lie at two site I' positions, on the 3-fold axis in the sodalite unit opposite D6Rs (see *Fig*. 3).

The distances between sites I and two I' are 2.01 and 2.58 Å. To avoid the very short distances where intercationic electrostatic repulsion should be severe, the two I' positions of the same D6R should not be occupied if its site I is filled. Accordingly, only (16–4) × 2 = 24 site I' positions should be available for cations per unit cell. This is in agreement with the number found at site I', 24.7(4).

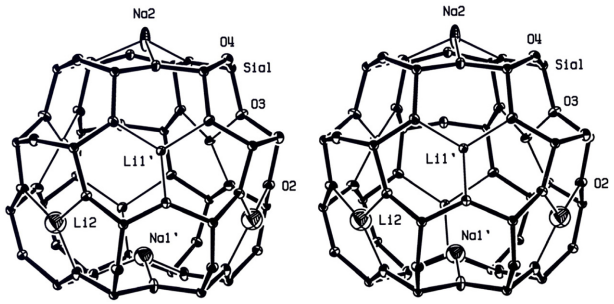


***Fig.* 3.** A stereoview of representative sodalite unit in dehydrated $|Li_{50}Na_{25}|[Si_{117}Al_{75}O_{384}]$-FAU. See the caption to *Fig*. 2 for other details.

The $Li^+$ ions at Li(I') are bonded by three O(3) oxygen atoms of the D6R at 1.926(5) Å, which are almost the same as the sum of the conventional ionic radii of $Li^+$ and $O^{2-}$, 0.59 + 1.32 (respectively) = 1.91 Å.[31,32]

The $Na^+$ ions at site I' are 2.083(12) Å from three O(3) framework oxygens. This distance is somewhat shorter than the sum of the corresponding ionic radii of $Na^+$ and

***Table* 5.** Displacements of atoms (Å) from 6-ring planes

| Positions | Sites | Displacement | |
|---|---|---|---|
| | | at O(3)[a] | at O(2)[b] |
| Na(I) | I | −1.71 | |
| Li(I') | I' | 0.30 | |
| Na(I') | I' | 0.87 | |
| Li(II) | II | | 0.23 |
| Na(II) | II | | 0.89 |

[a]A positive displacement indicates that the cation lies in a sodalite cavity; a negative displacement indicates that the cation lies in a D6R. (Na(I) centers D6Rs.) [b]A positive displacement indicates that the cation lies in a supercage.

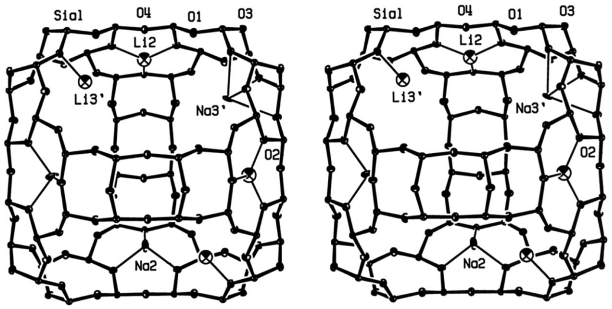


***Fig*. 4.** A stereoview of representative supercage in dehydrated $|Li_{50}Na_{25}|[Si_{117}Al_{75}O_{384}]$-FAU. See the caption to *Fig*. 2 for other details.

$O^{2-}$, 2.29 Å.[30] However, it is in agreement with previous results, Na(I')–O(3) = 2.12(7), 2.14(6), and 2.128(21) Å in fully dehydrated partially $Li^+$-exchanged zeolites Y.[17] This is attributed to the low occupancy number of $Na^+$ at site I'.

Each ion at Li(I') and Na(I') lies inside the sodalite cavity, 0.30 and 0.87 Å, respectively, from its three O(3) plane (see *Fig.* 3 and *Table* 5). The corresponding O(3)–Li(I')–O(3) and O(3)–Na(I')–O(3) bond angles are 117.7(3)° and 104.6(8)°, respectively.

About 20 $Li^+$ and 12 $Na^+$ ions per unit cell at Li(II) and Na(II), respectively, are located at site II opposite S6Rs in the supercage (see *Fig.* 4). These 32-fold positions are fully occupied by the $Li^+$ and $Na^+$ ions.

The $Li^+$ and $Na^+$ ions at Li(II) and Na(II), respectively, are coordinated by three O(2) oxygen atoms of the S6Rs at distances of 2.038(5) and 2.211(7) Å, respectively, which are in close agreement with the sum of the ionic radii of $Li^+$ and $O^{2-}$, 1.91 Å and $Na^+$ and $O^{2-}$, 2.29 Å.[30] While Li(II) extends 0.23 Å into supercage from its three O(2) plane, Na(II) extends, 0.89 Å, which is 0.66 Å much further than Li(II) (see *Fig*. 4 and *Table* 5).

The 11 $Li^+$ ions per unit cell are located at site III' in the supercages (see *Fig.* 4). These $Li^+$ ions bind strongly only to one oxygen atom, O(4), at 2.00(8) Å (see *Table* 4). This position was not found in previous studies. No $Li^+$ ions were found at site III as observed in the structure of fully dehydrated $Li_{72}Na_3$-Y.[17]

The thermal parameters of the $Li^+$ ions at site III' are much higher than sites I' and II, as in previous work (see *Table* 3),[17] suggesting the presence of further positional disorder at Li(III'), which could not be resolved in this work. This high thermal parameters may be a consequence of the combined effects of the low coordination number, one, and high mobility of $Li^+$ ion at this site.

The remaining 4 $Na^+$ ions in the supercage at site III' are 4-coordinated by framework oxygen atoms, two O(1) atoms at 2.77(4) Å and two O(4) atoms at 2.60(3) Å (see *Table* 4). These distances are much longer than the sum of the $Na^+$ and $O^{2-}$ radii, 2.29 Å.[30] However, these long interaction distances were also observed in the structures of fully dehydrated $Na_{75}$-Y,[33] $Li_{63}Na_{12}$-Y, $Li_{60}Na_{15}$-Y, and $Li_{54}Na_{21}$-Y.[17]

Generally, the zeolite framework adapts itself to the size of the cation, leading to remarkable distortions of the 6-rings windows in the case of $Li^+$-exchanged zeolites due to small size and strong electric filed of $Li^+$ ion.[12–14,17]

In this structure, T-O-T angles at O(2) and O(3), 132.19(18)° and 126.79(18)°, respectively, are much smaller than that in fully dehydrated Na-Y,[33] 145.3(2)°and 140.4(2)°. This observation is an excellent agreement with the result of previous works.[12–14,17] It seems clear that zeolite framework is under some strain as a result of much smaller size and higher interaction of $Li^+$ ion than $Na^+$ ion: it strongly pulls the oxygens atoms of its 6-rings toward the 6-ring centers.

In the case of single-crystal structure of $Li^+$-exchanged zeolite X (Si/Al = 1.09),[15] the loss of the crystallinity was found due to the distortions of the zeolite framework during dehydration. However, crystallographic evidence for indication of the loss of crystallininty is not observed in this structure. It is strongly correlated with relatively higher structural stability of $Li^+$-exchanged zeolite Y than X at high temperature.

In this structure, $Li^+$ ions are preferentially located at sites I' and II and the remaining $Li^+$ ions occupy site III' as found in previous structural studies in fully dehydrated Li-LSX,[13,14] Li-X,[12,14] and Li-Y.[17] However, Li(III') position is quite different from previous studies.[12–14,17] Li(III') is close to the side of a 12-ring in the supercage by the closest oxygen atom O(4) as shown in *Fig*. 4. These $Li^+$ ions coordinate only to one oxygen atoms, O(4). This position is similar to the $Na^+$ ions in the structure of fully dehydrated $Na_{71}$-Y.[34] This is attributed to the high mobility of $Li^+$ ion in the supercage and local Si-Al order among T

***Table* 6.** Distibution of $Li^+$ and $Na^+$ ions of fully dehydrated partially $Li^+$-exchanged zelite Y

| Crystal | Site I | Site I' | | Site II | | Site III' | | Total Cations | | | % IE[a] |
|---|---|---|---|---|---|---|---|---|---|---|---|
| | $Na^+$ | $Li^+$ | $Na^+$ | $Li^+$ | $Na^+$ | $Li^+$ | $Na^+$ | Total $Li^+$ | Total $Na^+$ | Total Cations | |
| $Li_{54}Na_{21}$-Y[b] | 2 | 24 | 4 | 24 | 8 | 6[c] | 7 | 48 | 21 | 69 | 72 |
| $Li_{50}Na_{25}$-Y[d] | 4 | 19 | 5 | 20 | 12 | 11 | 4 | 50 | 25 | 75 | 67 |

[a]Percent ion exchange of $Li^+$. [b]Reference 17. Crystal prepared from aqueous solution at 333 K. [c]These $Li^+$ ions were not found crystallographically, presumably because of their low occupancies and scattering powers. They are needed for charge balance. [d]This work. Crystal prepared from aqueous solution at 293 K.

atoms in zeolite framework.

Recently, the structure of fully dehydrated partially $Li^+$-exchanged zeolite Y from aqueous solution at 333 K was determined by single-crystal synchrotron X-ray diffraction techniques.[17] In this structure, 48 $Li^+$ ions were found at sites I' and II, 24 at each, and 21 $Na^+$ ions at sites I, I', II, and III'.

When the structures of fully dehydrated $Li_{54}Na_{21}$-Y[17] and $Li_{50}Na_{25}$-Y (this work) are compared, it can be seen that the site II is full and sites I/I' are full according to the rule $n_I + n_{I'}/2 = 16$ by $Li^+$ and $Na^+$ ions and remaining $Na^+$ ions are located at sites III' in both structures (see *Table* 6). In the structure of $Li_{50}Na_{25}$-Y, remaining $Li^+$ ions of the expected 75 cations per unit cell to balance the negative charge of the framework were found at site III'. These cations were not found at either of the sites, III or III' in the structure of $Li_{54}Na_{21}$-Y.

Generally, the extent of cation exchange increases with increasing ion-exchange temperature due to the greater mobility of cation at higher ion-exchange temperature. A similar trend is seen when the structures of $Li_{54}Na_{21}$-Y[17] and $Li_{50}Na_{25}$-Y are compared.

With increasing ion-exchange temperature from 293 K (this work) to 333 K ($Li_{54}Na_{21}$-Y),[17] the $Li^+$ exchange level increases from 67 to 72%. The number of $Na^+$ ions at sites I, I', II, and III' decreased with increasing $Li^+$-exchanged level in both structures of dehydrated $Li^+$-exchanged zeolite Y.

As mention above, the complete $Li^+$-exchange from conventional aqueous solution did not occur in the zeolite Y. This is attributed to the large polarity of the ion-exchange solution relative to polarity of zeolite Y. Water is high polar. Therefore, $Li^+$ ion exchange into zeolite Y from aqueous solution is discouraged due to the higher Si/Al ratio of the zeolite framework, the smaller negative charge density of the framework, and the resulting electric fields.[17]

## SUMMARY

$Li^+$-exchanged zeolite Y was prepared from aqueous 0.1 M $Li(NO_3)$ solution by dynamic ion-exchange method at 293 K, followed by vacuum dehydration at 673 K and $1.0 \times 10^{-6}$ Torr. The crystal structure was determined by single-crystal synchrotron X-ray diffraction techniques. The complete exchange of $Li^+$ into zeolite Y was not achieved because $Li^+$ ion has high hydration energy in water. The degree of $Li^+$ ion exchange in this structure is 67%. In the crystallographic study, 50 $Li^+$ ions per unit cell are found at sites I', II, and III' and 25 $Na^+$ ions at sites I, I', II, and III'. The $Li^+$ for $Na^+$ ions fill preferentially at sites I' and II and the remaining $Li^+$ ions occupy sites III'. Li(III') is close to the side of a 12-ring in the supercage by the closest oxygen atom O(4).

**Acknowledgments.** The authors are grateful to the staff at beamline 6B MXI of the Pohang Light Source, Korea, for their assistance during data collection. This work was carried out with the support of 'Cooperative Research Program for Agriculture Science & Technology Development (Project No. PJ008316)' Rural Development Administration, Republic of Korea.

## REFERENCES

1. Breck, D. W. *Zeolite Molecular Sieves*; Wiley: New York, 1974.
2. Seo, S. M.; Kim, G. H.; Lee, S. H.; Bae, J. S.; Lim, W. T. *Bull. Korean Chem. Soc*. **2009**, *30*, 1285.
3. Warzywoda, J.; Valcheva-Traykova, M.; Rossetti, Jr., G. A.; Bac, N.; Joesten, R.; Suib, S. L.; Sacco, Jr., A. *J. Cryst. Growth* **2000**, *220*, 150.
4. Baerlocher, C.; Meier, W. M.; Olsen, D. H. *Atlas of Zeolite Framework Types*, 5th ed.; Elsevier: Amsterdam, 2001.
5. Kwon, J. H.; Jang, S. B.; Kim, Y.; Seff, K. *J. Phys. Chem.* **1996**, *100*, 13720.
6. Seff, K. *In Studies in Surface Science and Catalysis*; Elsevier: New York, **1996**, *102*, 267.
7. Chao, C.; Sherman, J.; Mullhaupt, J. T.; Boliner, C. M. Mixed Ion-exchanged Zeolites and Processes for The use Thereof in Gas separations. U.S. Patent 5,413,625, 1995.
8. Gaffney, T. R. *Solid State and Materials Science* **1996**, *1*, 69.
9. Feuerstein, M.; Accardi, R. J.; Lobo, R. F. *J. Phys. Chem.*

*B* **2000**, *104*, 10281.
10. Zhu, J.; Mosey, N.; Woo, T.; Huang, Y. *J. Phys. Chem. C* **2007**, *111*, 13427.
11. Pitchumani, K.; Ramamurthy, V. *Tetrahedron* **1996**, *37*, 5279.
12. Forano, C.; Slade, R. C. T.; Krogh Andersen, E.; Krogh Andersen, I. G.; Prince. E. *J. Solid State Chem.* **1989**, *82*, 95.
13. Plevert, J.; Di Renzo, F.; Fajula, F. *J. Phys. Chem. B* **1997**, *101*, 10340.
14. Feuerstein, M.; Lobo, R. F. *Chem. Mater*. **1998**, *10*, 2197.
15. Shepelev, Y. F.; Anderson, A. A.; Smolin, Y. I. *Zeolites* **1990**, *10*, 61.
16. Kim, H. S.; Ko, S. O.; Lim, W. T. *Bull. Korean Chem. Soc.* **2012**, *33*, 3303.
17. Kim, H. S.; Bae, D.; Lim, W. T.; Seff, K. *J. Phys. Chem. C* **2012**, *116*, 9009.
18. Lim, W. T.; Seo, S. M.; Wang, L. Z.; Lu, G. Q.; Heo, N. H.; Seff, K. *Microporous Mesoporous Mater*. **2010**, *129*, 11.
19. Otwinowski, Z.; Minor, W. *Methods Enzymol*. **1997**, *276*, 307.
20. Bruker-AXS, *XPREP*, version 6.12, Program for the Automatic Space Group Determination. Bruker AXS Inc.: Madison, WI, 2001.
21. Sheldrick, G. M. *SHELXL97*, Program for the Refinement of Crystal Structures. University of Gottingen: Germany; 1997.
22. Lim, W. T.; Choi, S. Y.; Choi, J. H.; Kim, Y. H.; Heo, N. H.; Seff, K. *Microporous Mesoporous Mater*. **2006**, *92*, 234.
23. Doyle, P. A.; Turner, P. S. *Acta Crystallogr*., Sect. *A* **1968**, *24*, 390.
24. *International Tables for X-ray Crystallography*; Ibers, J. A.; Hamilton, W. C., Eds.; Kynoch Press: Birmingham: England, 1974; Vol. IV, pp 71-98.
25. Cromer, D. T. *Acta Crystallogr*. **1965**, *18*, 17.
26. *International Tables for X-ray Crystallography*; Ibers, J. A.; Hamilton, W. C., Eds.; Kynoch Press: Birmingham, England, 1974; Vol. IV, pp 148-150.
27. Loewenstein, W. *Am. Mineral*. **1954**, *39*, 92.
28. Smith, J. V. *Molecular Sieve Zeolites*-I; Flanigen, E. M.; Sand, L. B., Eds.; Advances in Chemistry Series: American Chemical Society, Washington, D. C., 1971; Vol. 101, pp 171-200.
29. Song, M. K.; Kim, Y.; Seff, K. *J. Phys. Chem. B* **2003**, *107*, 3117.
30. *Handbook of Chemistry and Physics*, 70th ed.; CRC Press: Cleveland, OH, 1989/1990; pp F-187.
31. Wozniak, A.; Marler, B.; Angermund, K.; Gies, H. *Chem. Mater.* **2008**, *20*, 5968.
32. *Handbook of Chemistry and Physics*, 77th ed.; CRC Press: Boca Raton, FL, 1996/1997; pp 12-14.
33. Su, H.; Kim, H. S.; Seo, S. M.; Ko, S. O.; Suh, J. M.; Kim, G. H.; Lim, W. T. *Bull. Korean Chem. Soc.* **2012**, *33*, 2785.
34. Seo, S. M.; Kim, G. H.; Lee, H. S.; Ko, S. O.; Lee, O. S.; Kim, Y. H.; Kim, S. H.; Heo, N. H.; Lim, W. T. *Anal. Sci.* **2006**, *22*, 209.